ACCELERATOR PHYSICS CHALLENGES OF X-RAY FEL SASE SOURCES*

P. Emma†, SLAC, Stanford, CA 94309, USA

Abstract

A great deal of international interest has recently focused on the design and construction of free-electron lasers (FEL) operating in the x-ray region (~1 Å). At present, a linac-based machine utilizing the principle of self-amplified spontaneous emission (SASE) appears to be the most promising approach. This new class of FEL achieves lasing in a single pass of a high brightness electron beam through a long undulator. The requirements on electron beam quality become more demanding as the FEL radiation wavelength decreases, with the 1-Å goal still 3-orders of magnitude below the shortest wavelength operational SASE FEL (TTF-FEL at DESY [1]). The sub-picosecond bunch length drives damaging effects such as coherent synchrotron radiation, and undulator vacuum chamber wakefields. Unlike linear colliders, beam brightness needs to be maintained only over a small 'slice' of the bunch length, so the concepts of bunch-integrated emittance and energy spread are less relevant than their high-frequency (or 'time-sliced') counterparts, also adding a challenge to phase space diagnostics. Some of the challenges associated with the generation, preservation, measurement, and stability of high-brightness FEL electron beams are discussed here.

1 INTRODUCTION

The promise of x-ray SASE FELs, as compared with 3rd generation light sources, is nearly ten orders of magnitude increase in peak photon brightness and two orders of magnitude reduction of pulse length. This remarkable step in performance is made possible with the advent of the photocathode rf electron gun [2], and recent progress in beam brightness preservation for linear colliders [3], [4], [5]. Two major projects, *LCLS* at SLAC [6] and *TESLA-FEL* at DESY [4], are currently in an advanced stage of planning, with similar, longer wavelength projects in Japan [7], England [8], Germany [9], and Italy [10] at the conceptual design stage.

For these 4th generation linac-based FELs, the common requirement is a very high brightness electron bunch with typical parameters: 0.5-1 nC charge, 1-3 mm-mrad normalized emittance, 2-5 kA peak current, 0.01-0.05% relative energy spread, and 3-50 GeV electron energy. In contrast to linear colliders, where particle collisions effectively integrate over the entire bunch length, the x-ray FEL 'integrates' only very short fractions of the electron bunch length. The integration length is given by the FEL slippage length, which is the electron-to-photon longitudinal slippage over the length of undulator prior to SASE saturation, and is the number of undulator periods multiplied by the radiation wavelength. For 1-Å radiation and typically several thousand undulator periods of a few centimeters, the slippage length is less than one micron. This corresponds to ~1% of the bunch length, which in fact makes the job of emittance preservation easier, but also brings new demands for beam diagnostics. With this difference in mind, some of the various technical challenges related to beam brightness generation, preservation, and diagnostics are described.

2 SASE FEL REQUIRMENTS

The SASE FEL requires an electron beam with 'slice' transverse normalized rms emittance roughly estimated by

$$\varepsilon_N <\sim \gamma\frac{\lambda_r}{4\pi}, \qquad (1)$$

where γ is the electron energy, E, in units of rest mass ($\gamma = E/mc^2$), and λ_r is the radiation wavelength (~1 Å). For $\gamma \approx 3\times10^4$, the emittance requirement is $\varepsilon_N <\sim 1\ \mu$m ($\varepsilon_x \approx \varepsilon_y$). This is a challenging level for electron sources at ~1-nC, but can be eased a bit by using longer undulators.

At the same time, the 'slice' rms e^- relative energy spread should be

$$\frac{\sigma_E}{E} < \rho \approx \frac{1}{4}\left(\frac{1}{2\pi^2}\frac{I_{pk}}{I_A}\frac{\lambda_u^2}{\beta\varepsilon_N}\left(\frac{K}{\gamma}\right)^2\right)^{1/3}, \qquad (2)$$

where ρ is the FEL parameter, λ_u the undulator period, K (assumed >> 1 here) the 'planar' undulator parameter ($K \equiv eB\lambda_u/2\pi mc$), B peak undulator field, I_{pk} peak e^- current, $I_A \approx 17$ kA, and β the mean beta function in the undulator. For $K \approx 4$, $\gamma \approx 3\times10^4$, $I \approx 4$ kA, $\beta \approx 20$ m, $\lambda_u \approx 3$ cm, then $\sigma_E/E < 0.05\%$ at $\varepsilon_N \approx 1.5\ \mu$m.

The gain-length of the FEL, typically underestimated in this 1D-model, is given by

$$L_g \approx \frac{\lambda_u}{4\pi\sqrt{3}\rho}. \qquad (3)$$

For SASE saturation, the undulator length must be $L_u > 20\cdot L_g$, so L_g, must be minimized and therefore I_{pk} maximized while preserving the transverse emittance. After accommodating some reasonable emittance growth, various undulator imperfections, and limited machine stability, plus a 3D-model, the needed undulator length can quickly stretch well beyond 100 m. The simultaneous requirement of high peak current, small energy spread, and small transverse emittance presents a significant challenge for the accelerator design.

* Work supported by DOE contract DE-AC03-76SF00515.
† Emma@SLAC.Stanford.edu

3 INJECTOR

The injector is typically based on an rf photocathode gun which rapidly accelerates the photo-electrons from the cathode in order to minimize the effects of space-charge forces on beam brightness. A solenoid magnet immediately after the cathode is used to focus the beam into the next accelerating section and accomplishes a compensation of the space-charge induced correlated emittance growth [11], [12]. The challenge is to extract ~1-nC charge in a ~100-A bunch with transverse normalized emittance ~1 μm. These levels have not yet been simultaneously achieved to date, but most measurements reflect the 'projected' emittance. Some measurements have indicated sub-micron slice emittance levels [13], [14], but at a reduced charge of 0.1-0.3 nC.

An alternate approach to high-brightness electron beam generation is being pursued in Japan using a low emittance HV-pulsed gun with a CeB_6-cathode [7] and a reduced bunch charge level of 0.1 to 0.5 nC.

In addition to generating the high brightness electron beam, the injector must serve as a stable base to operate the FEL. The cathode-illumination laser must be stable in timing, with respect to linac RF phase, to sub-picosecond levels, and laser power at the cathode (the electron bunch charge) must be stable to typically a few percent in the UV. These levels need to be achieved over time scales of a few seconds. Longer time scales will be accommodated by including timing and charge feedback systems.

4 LINAC

The linac accelerates and compresses the electron bunch, while preserving beam brightness. Acceleration reduces the geometric emittance, more closely satisfying Eq. (1), while compression increases the peak current, fulfilling Eq. (2). Bunch compression is typically accomplished by accelerating at an off-crest rf phase, providing a nearly linear energy 'chirp' (correlation) along the bunch length. A series of dipole magnets (usually a simple 4-dipole chicane) is used to generate an energy dependent path length so that the chirped bunch compresses in length.

One of the most challenging issues associated with magnetic bunch compression is the effect of coherent synchrotron radiation (CSR) in the bends. An electron bunch following a curved trajectory in a bend magnet will radiate energy. For wavelengths shorter than the bunch length this radiation will be coherent and at power levels greater, by the number of electrons in the bunch (N), than the incoherent component. Figure 1 shows the radiation spectrum for the final bends of the *LCLS* 1st-stage (BC1) and 2nd-stage (BC2) compressors. The solid curves show the coherent radiation increases by $N \approx 6\times10^9$ over the incoherent radiation (dashed), at wavelengths longer than the final rms bunch length (200 μm for BC1 and 20 μm for BC2). The incoherent power drops off as $\lambda^{-1/3}$.

The radiation field from the back of the bunch may catch up to the head of the bunch by propagating along the chord of the trajectory. The radiation field may be strong enough to alter the energy of leading electrons causing a trajectory change through the bends. The different trajectory distortions for different sections of the bunch length becomes a projected emittance growth in the bend plane, but not necessarily a slice emittance growth. Slice emittance growth, however, can also be generated by the incoherent radiation at high energy, or by the transverse gradient of the CSR longitudinal wakefield across a bunch with significant transverse extent [15].

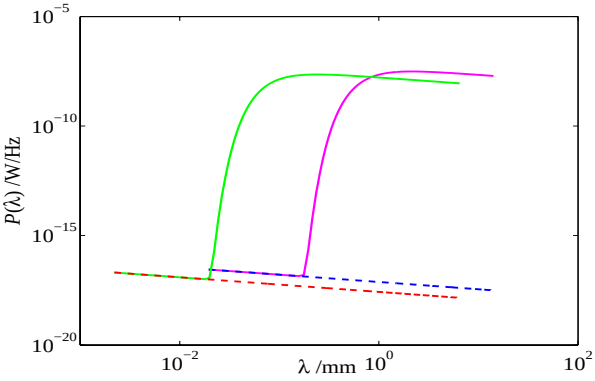

Figure 1: CSR power spectrum for *LCLS* BC1 (magenta & blue) and BC2 chicanes (green & red). Dashed curves (blue & red) show only the incoherent radiation (~ $\lambda^{-1/3}$).

The compressors must be designed with these detrimental effects in mind. Various design considerations have been proposed to mitigate the emittance growth [16], [17], [18].

In addition to the projected emittance growth, tracking studies [19] have also revealed a potentially more damaging CSR instability which can develop for very cold beams. Small density modulations on the current or energy profiles can be magnified by the CSR longitudinal wakefield, depending on the wavelength of the modulation, the beam's incoherent energy spread, and the slice emittance in the bend-plane [20], [21], [22].

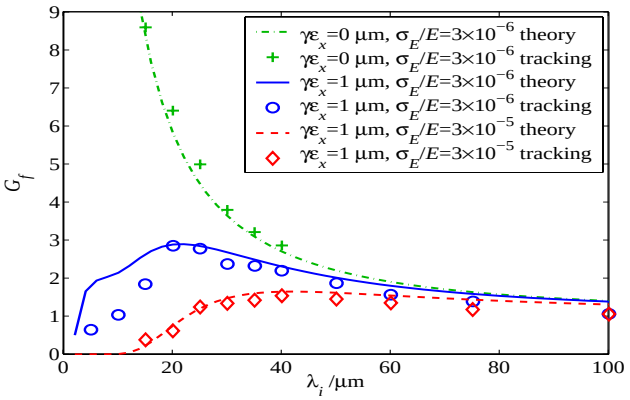

Figure 2: CSR microbunching gain, G_f, versus modulation wavelength, λ_i, at entrance to *LCLS* BC2 chicane for various 'slice' emittance and 'slice' energy spread values.

Figure 2 shows gain versus modulation wavelength at the *LCLS* BC2 chicane entrance calculated with tracking and in theory from ref. [20]. Particle tracking of the *LCLS*

shows large amplification through the series of four bend systems, two of which are bunch compressor chicanes. The *LCLS* layout is shown schematically in Figure 3.

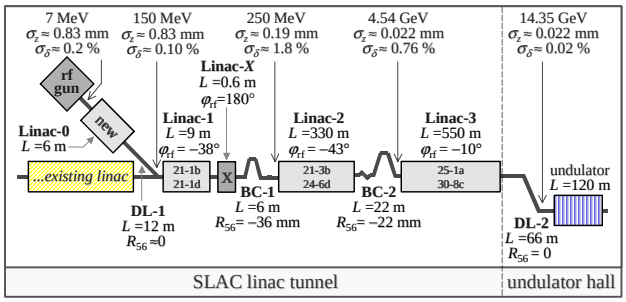

Figure 3: Layout of LCLS accelerator and compressors.

The microbunching effect is even more severe for the double-chicane compressor initially proposed for the *LCLS* BC2 [16], forcing a design change to a single-chicane. The single-chicane produces more projected emittance growth, but less microbunching, the latter being a more significant effect for the FEL.

The strong microbunching at high frequencies can increase the 'slice' emittance and the 'slice' energy spread. The effect at 14.3 GeV, at the end of the *LCLS*, is shown on the top 3-plots of Figure 4. The microbunching is strongly damped by including a short, one-period superconducting wiggler magnet prior to BC2 at 4.5 GeV (see bottom 3-plots of Figure 4). The wiggler increases the rms incoherent energy spread from 3×10^{-6} to 3×10^{-5} at 4.5 GeV, which generates a slippage across the chicane effectively smearing out the microbunching. The same damping can be achieved by increasing the bend plane slice emittance, but such freedom is not available in most emittance dominated SASE x-ray FEL's, since Eq. (1) is already violated. On the other hand, Eq. (2) is usually well satisfied, so there is head-room to add energy spread without changing the FEL gain.

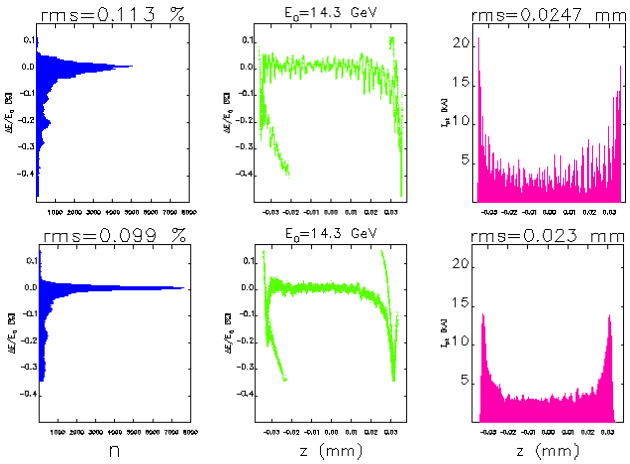

Figure 4: Final longitudinal phase space at undulator entrance (14.35 GeV) both without (top) and with (bottom) superconducting pre-BC2 wiggler switched on.

Figure 5 shows simulated horizontal, *x*, versus longitudinal, *z*, position after CSR effects in *LCLS* with damping wiggler on. The projected emittance growth is seen as simple 'steering' of the bunch head (left) and tail.

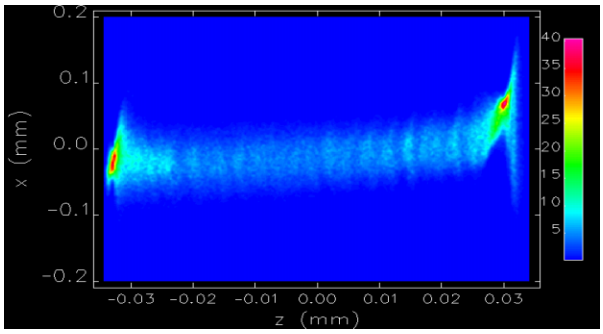

Figure 5: Simulated horizontal vs. longitudinal position after CSR effects in *LCLS* with damping wiggler on.

The large compression factor required (~50) also amplifies non-linear effects due to the sinusoidal shape of the rf, longitudinal wakefields of the rf structures, and the compressor's 2nd-order path length dependence on energy. A wakefield-induced example is clearly evident in the sharp 'horns' of the temporal distributions in Figure 4 (right-side plots). These sharp current spikes can further amplify CSR effects.

In some cases it is possible to compensate the non-linearities by including a higher harmonic rf accelerating section. This is such a natural solution that it has been independently proposed for the first compressor in *TESLA* [23] and the *LCLS* projects [24], and also for the *TTF-FEL*, and at Boeing [25]. In *TESLA*, a 3rd harmonic of *L*-band is used ($3f_L \approx 3.9$ GHz), while *LCLS* uses an existing NLC *X*-band structure, which is a 4th harmonic of *S*-band ($4f_S \approx 11.4$ GHz). By operating at or near the decelerating crest phase of the harmonic section with ~20 MV, both the 2nd-order curvature of the RF and the 2nd-order compression effects can be completely compensated, eliminating spikes in the compressed current distribution after the first compressor stage (BC1). This is much more difficult to compensate in the *LCLS* BC2, where strong longitudinal wakefields of the *S*-band structures and a non-uniform current profile generate a 3rd-order effect.

The differences in the *TESLA* and *LCLS* accelerator designs are most striking with regard to the accelerating rf. *LCLS* uses the existing SLAC linac with its *S*-band rf, while *TESLA* employs superconducting *L*-band rf. The accelerating gradients are similar at 18-25 MV/m, but the wakefield strengths are very different, introducing some advantages and disadvantages for each design.

Certainly the greatly reduced transverse wakefield of the *TESLA* design is a significant advantage, as is the lack of a strong longitudinal wakefield, which can otherwise result in the *LCLS* current spikes shown in Figure 4. But there is also a more subtle advantage to the strong longitudinal wakefield in the *LCLS*. In both machines the beam in BC2 is under-compressed, leaving a large time-correlated energy spread along the bunch. The strong longitudinal *S*-band wakefield can be used to completely cancel this linearly correlated energy spread prior to the undulator entrance (see center plots of Figure 4). For

TESLA, the absence of a wakefield means that this post-compression correlated energy spread must be kept to a minimum, since it persists and will introduce an undesirable frequency chirp to the FEL radiation. Keeping the energy spread to a minimum, and still compressing the bunch, forces stronger compressor bends, further intensifying CSR effects. In fact, the momentum compaction, R_{56}, for BC1 is 3-times larger in *TESLA* than in *LCLS*, and similarly for BC2 the *TESLA* value is 2-times larger (with a 3rd compression stage in *TESLA*).

It appears that the ideal machine would use superconducting *L*-band acceleration up to the final compressor, and then switch to conventional *S*-band. The *L*-band eliminates transverse wakefields, which are only significant while the bunch is still long, and mitigates longitudinal wakefield distortions prior to compression. Finally, the *S*-band provides a way to remove the correlated energy spread, allowing weaker compressors. This might be the best of both machines.

A less conventional approach to bunch compression is also being pursued at INFN. A new method based on a rectilinear compressor scheme, utilizing the bunching properties of slow waves, has been recently proposed to avoid CSR effects [26]. Such a scheme may allow, simultaneously, a small transverse emittance and a high peak current from the injector, without the deleterious effects of CSR in a strong magnetic bunch compressor.

Finally, it is possible to measure the bunch length, 'slice' emittance, and 'slice' energy spread of even the compressed bunch by using a transverse rf deflecting cavity. The deflector 'streaks' the bunch vertically so that the vertical beam size measured on an intercepting screen indicates the bunch length. Scanning a quadrupole while slicing the beam on the screen vertically allows a slice emittance measurement, and including a screen at a point with dispersion allows slice energy spread measurement. Even a 20-μm rms bunch length at 6 GeV can be measured in this way using a 20-MV S-band deflector at the 1-μm emittance levels needed for the FEL [27].

5 UNDULATOR

To accommodate SASE saturation at ~1 Å, the SASE x-ray FEL undulator is typically quite long (120 m for the *LCLS*, and up to 320 m for the *TESLA* FEL). The trajectory requirements for such an undulator are very demanding. An imperfect trajectory will generate electron/x-ray phase slippage and loss of spatial overlap, both of which reduce the gain.

The undulator needs focusing to keep the beam size nearly constant. Quadrupole magnets inserted between undulator sections are typically used for this purpose. The quadrupoles must then be aligned very precisely or the trajectory will not be straight enough. Beam position monitors (BPMs) and steering can be used to correct the effects of misaligned quadrupoles, but the BPMs must be well aligned. For radiation wavelength λ_r (≈ 1.5 Å), quadrupole spacing L (≈ 3.5 m), and number of undulator-sections n (= 33), the BPM alignment requirements (net phase slip $<\pi$) are estimated by [28]

$$\left\langle \Delta x^2 \right\rangle^{1/2} < \sqrt{\frac{\lambda_r L}{2n}} \,. \tag{4}$$

For the *LCLS*, this requirement is $\langle \Delta x^2 \rangle^{1/2} < 3$ μm. Such a level is not achievable using survey methods, so a beam-based procedure is applied to align the quadrupoles and the BPMs [29], [30]. Figure 6 shows the results of simulation of beam-based alignment for the *LCLS*. The final trajectory rms is 2-3 μm achieved using 1-μm resolution BPMs and scanning the beam energy over a wide range (5-14 GeV). The techniques are very reliant on BPM resolution and stability. BPMs must be built to accommodate 1-μm rms resolution and their readback offsets must not drift by more than 1-2 μm over the 1-2 hour period required to perform the procedure. Drifts due to thermal variations need to be well controlled.

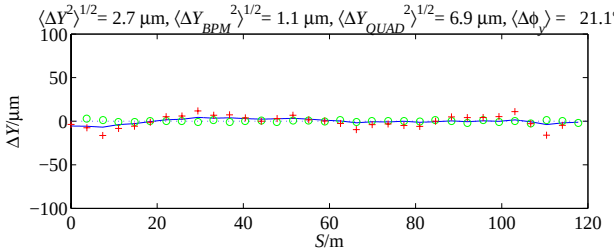

Figure 6: Final simulated *LCLS* undulator trajectory after three passes of the beam-based alignment procedure (solid: trajectory, O: BPM readbacks, +: quadrupole pos.).

Longitudinal wakefields are also an issue in the undulator. An initial correlated energy spread at undulator entrance simply generates a frequency chirped x-ray beam. But energy spread generated within the undulator of order of the FEL parameter ρ, changes the FEL resonance condition during the exponential gain regime and can have a significant impact on the x-ray output power and pulse shape.

The most significant mechanism is the resistive-wall (RW) wakefield [31], which shifts the mean energy of the various slices differently, increasing the projected energy spread. For a gaussian bunch with N (≈ 6×10^9) electrons in a cylindrically symmetric pipe of radius a, the rms relative energy spread is increased by

$$\left(\frac{\sigma_E}{E}\right)_{RW} \approx (0.22)\frac{e^2 c N L_u}{\pi^2 a E \sigma_z^{3/2}}\sqrt{\frac{Z_0}{\sigma}} \,, \tag{5}$$

where $Z_0 \approx 377\ \Omega$, σ is conductivity, and σ_z is the rms bunch length. For $a \approx 2.5$ mm, $\sigma_z \approx 20$ μm, $E \approx 15$ GeV, $L_u \approx 120$ m, and a copper pipe ($\sigma \approx 5.9\times10^7\ \Omega^{-1}\cdot m^{-1}$), the energy spread is 0.06% (≈ ρ). A larger radius helps, but it becomes difficult to produce a strong enough undulator field (K), so the undulator length must be increased, further increasing the wake. This effect limits the final bunch length, which otherwise might be further compressed to overcome emittance limitations in the gun.

The RW wakefield must be evaluated over the 'real' non-gaussian temporal bunch distribution and the evolving energy spread included in the SASE FEL gain calculations. This has been included in the computer code *Genesis 1.3* [32]. For the LCLS, the power reduction due to undulator wakefields is ~35%. Figure 7 shows the *LCLS* FEL output power versus distance along the undulator both with and without wakefields for a 1-nC and a 0.2-nC charge, and for 1.5-Å and 15-Å radiation. In addition to the RW wakefield, a vacuum chamber wall surface roughness wakefield can arise. Calculations for typical surfaces show this effect to be small [33].

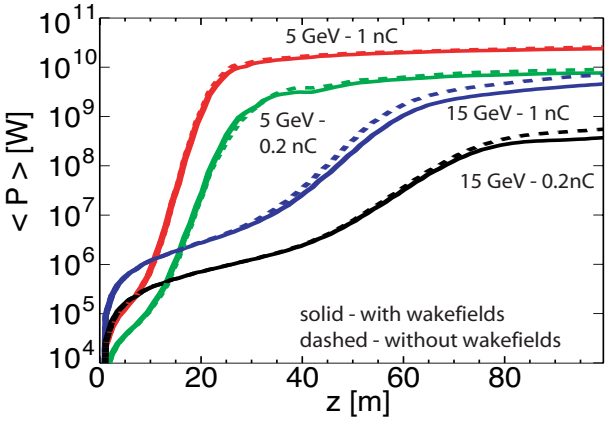

Figure 7: LCLS FEL output power vs. distance along the undulator with (solid) and without (dash) wakefields [32].

6 REFERENCES

[1] J. Rossbach et.al., NIM. A 475:13-19, 2001.

[2] R. Scheffield, "Photocathode RF Guns", Physics of Particle Accelerators, AIP Vol. 184, pp. 1500-1531.

[3] P. Emma, "The Stanford Linear Collider", PAC-1995, Dallas, TX, USA, May 1-5, 1995.

[4] "TESLA TDR", DESY 2000-011, March 2001.

[5] "Zeroth-Order Design Report for the Next Linear Collider", *SLAC Report 474*, May 1996.

[6] "LCLS CDR", SLAC-R-593, April 2002.

[7] T. Shintake et al., "SPring-8 SASE-FEL Project in Japan", EPAC-2002, Paris, France, June 3-7, 2002.

[8] J.A. Clarke, et al., "Prospects for a 4th Generation Light Source for the UK", PAC-2001, Chicago, IL.

[9] M. Abo-Bakr et al., "The Bessy FEL Project", NIM A483:470-477, 2002.

[10] L. Serafini, "An R&D Program for a High Brightness Electron Beam Source at LNF", EPAC-2002, Paris, France, June 3-7, 2002.

[11] B. E. Carlsten, "New Photelectric Injector Design for the Los Alamos National Laboratory XUV FEL Accelerator", Nucl. Instr. Meth. A 285, 313, 1985.

[12] L. Serafini, J. B. Rosenzweig, "Envelope Analysis of Intense Relativistic Quasilaminar Beams in RF Photoinjectors", Phys. Rev. E 55, 7565, 1997.

[13] W. Graves et. al., "Experimental Study of Sub-psec Slice Electron Beam Parameters in a Photoinjector", submitted to FEL-2002, Argonne, IL, Sep. 2002.

[14] D. H. Dowell et. al., "Slice Emittance Measurements at the SLAC Gun Test Facility", submitted to FEL-2002, Argonne, IL, Sep. 2002.

[15] M. Dohlus et al., "Uncorrelated Emittance Growth in the TTF-FEL Bunch Compression Sections Due to Coherent Synchrotron Radiation and Space Charge Effects", EPAC-2000, Vienna, Austria.

[16] P. Emma, R. Brinkmann, "Emittance Dilution Through Coherent Energy Spread Generation In Bending Systems", PAC-97, Vanc., BC, Canada.

[17] M. Dohlus, A. Kabel, T. Limberg, "Optimal Beam Optics in the TTF-FEL Bunch Compression Sections: Minimizing The Emittance Growth", PAC-99, New York, NY, 29 March - 2 April, 1999.

[18] A. Loulergue, A. Mosnier, "A Simple S-chicane for the Final Bunch Compressor of TTF-FEL", EPAC-2000, Vienna, Austria, 2000.

[19] M. Borland et al., "Start-to-End Simulation of Self-Amplified Spontaneous Emission Free-Electron Lasers from the Gun through the Undulator", FEL-2001, Darmstadt, Germany, August 2001.

[20] S. Heifets et al., "CSR Instability in a Bunch Compressor", SLAC-PUB-9165, March 2002.

[21] E. L. Saldin, et al., "Longitudinal Phase Space Distortions in Magnetic Bunch Compressors", FEL-2001, Darmstadt, Germany, August 2001.

[22] Z. Huang, K.-J. Kim, "Formulae for CSR Microbunching in a Bunch Compressor Chicane", submitted to *Phys. Rev. Spec. Topics – Acc. and Beams*, April 2002.

[23] P. Piot et. al., "Conceptual Design for the XFEL Photoinjector", DESY TESLA-FEL 01-03, 2001.

[24] P. Emma, "X-Band RF Harmonic Compensation for Linear Bunch Compression in the LCLS", LCLS-TN-01-1, Nov. 2001.

[25] D. Dowell et al., "Magnetic Pulse Compression Using a Third-Order Linearizer", PAC-1995, Dallas, TX, USA, 1995.

[26] M. Ferrario et al, "Beam Dynamics Study of an RF Bunch Compressor for High Brightness Beam Injectors", EPAC-2002, Paris, France, 2002.

[27] R. Akre et al., "A Transverse RF Deflecting Structure for Bunch Length and Phase Space Diagnostics", LCLS-TN-00-12, Aug. 2000.

[28] P. Emma, "Phase Slip in an Undulator with Pole and BPM Errors", PAC-2001, Chicago, IL, USA, 2001.

[29] P. Emma et. al., "Beam-Based Alignment of the LCLS FEL Undulator", FEL-98, Williamsburg, VA.

[30] B. Faatz, "Beam-Based Alignment of the TESLA Free Electron Laser Undulator", DESY TESLA-FEL 01-04, 2001.

[31] K.L.F. Bane, M. Sands, "The Short-Range Resistive Wall Wakefields," Micro Bunches Workshop, Upton, New York, September 28-30, 1995.

[32] S. Reiche, NIM A 429 (1999) 242.

[33] G. Stupakov, "Surface Roughness Impedance", *Physics of, and Science with, the X-ray Free Electron Laser*, Arcidosso, Italy, Sep. 2000.